Department of Physics and Astronomy
University of Heidelberg

Bachelor Thesis in Physics
submitted by

Sophia Milanov

born in Düsseldorf (Germany)

2016

Hunting for intermediate-mass black holes: a new action-based approach

This Bachelor Thesis has been carried out by Sophia Milanov at the
Max Planck Institute for Astronomy in Heidelberg
under the supervision of
Dr. Glenn van de Ven

Abstract

Hello, here is some text without a meaning. This text should show what a printed text will look like at this place. If you read this text, you will get no information. Really? Is there no information? Is there a difference between this text and some nonsense like “Huardest gefburn”? Kjift – not at all! A blind text like this gives you information about the selected font, how the letters are written and an impression of the look. This text should contain all letters of the alphabet and it should be written in of the original language. There is no need for special content, but the length of words should match the language.

Contents

1 Introduction **6**

2 Method & Theory **9**

2.1 Stellar population in GC 9
2.2 Kinematic profiles of globular clusters 10
2.3 Density & potential 10
2.4 Integrals of motion 10
2.5 Orbits & orbit integration 10
2.6 Actions 13

3 Analysis **15**

3.1 Description of the simulation 15
3.2 Investigation in phase space 15
3.2.1 Velocity dispersion 19
3.2.2 Anisotropy 19
3.2.3 Density profile 21
3.2.4 Potential 21
3.3 Investigations of orbits in action space 21
3.3.1 Orbits & actions 21
3.3.2 Integral of motions along orbits 21

4 Results & Discussion **24**

4.1 Signatures of intermediate mass black holes (IMBHs) in action space . . 24
4.2 Discussion & future perspectives 31

5 Conclusion **33**

6 Acronyms **34**

1 Introduction

Globular clusters (GCs) are self-gravitating, gas-free systems of maybe 10^5 to maybe 10^7 stars which are spherically grouped. There are about 150 of them in the Milky Way (MW). Since they are some of the oldest stellar populations in the universe (approximately 13 Gyr), they contain much information about the assembly history and evolution of the MW. Formerly seen as very simple spherical and isotropic stellar systems with only one stellar population, recent research revealed a much higher degree of complexity (that differ in the light-elements abundances). GCs are now known to host multiple stellar populations that challenge our understanding of their formation. Moreover, GCs now also appear dynamically complex, presenting deviations from spherical symmetry, anisotropy in velocity space and significant internal rotation.

Recent attention has been devoted to the search of IMBHs in the centre of GCs. These elusive black holes $10^3 M_\odot < M_\bullet < 10^4 M_\odot$ could be the missing link between stellar mass black holes ($M_\bullet < 100 M_\odot$) and super massive black holes (SMBHs, $M_\bullet > 10^5 M_\odot$) as they could represent the seed for the formation of SMBHs. Their search in the centre of GCs has partially been motivated by the extrapolation of the $M_\bullet - \sigma$-relation for galaxies, describing the relation between the mass of a central massive black hole and the velocity dispersion of its host galaxy.

The hunt of IMBHs in Galactic GCs has been primarily based on two methods: 1) detection of radio and X-ray emission due to the accretion of gas in the black hole; 2) detection of kinematic signatures in the central region of a GC. The first method proved to be difficult because the feeding of a black hole with gas is highly inefficient in a gas poor environment of Galactic GCs.

The kinematic detection of IMBHs is usually based on the analysis of the velocity-dispersion profile in the inner few arcseconds around the crowded centre of a GC in search for a rise of the dispersion. This requires a combination of high angular resolution and high spectral resolving power. For this reason the detection of IMBHs remains still highly controversial.

Currently there are two different kinematic methods trying to detect IMBHs: resolved kinematics & unresolved integrated light [bianchini 2015] **?** These methods often deliver significant different results when applied to the same GC. As an example there are the unresolved/integrated IFU kinematics which result in a signature of an IMBH for NGC 6388 (cusp in the velocity dispersion profile) and resolved/discrete kinematics which do not yield IMBHs (no cusp in the velocity dispersion profile).

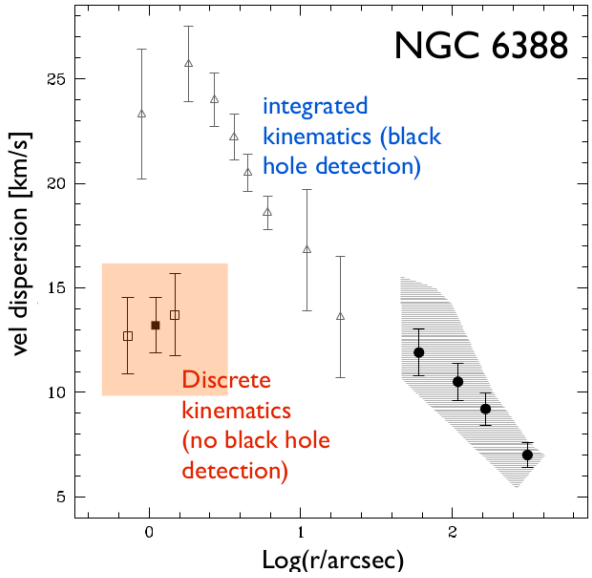

Figure 1: Velocity profile of NGC 6388 derived by the two different methods. We see a cusp given by the integrated kinematics method while there is no cusp with discrete kinematics. (**?**) and bianchini?

Given these controversial results that prevent us from drawing definite conclusions on the existence of IMBHs in Galactic GCs we propose to introduce a new approach to analyse the effects of an IMBH to the central kinematic of a GC. Our method consists in going beyond the traditional phase space analysis (i.e., analysis of velocity dispersion profiles), by exploiting the orbital information of the stars. Our expectation is that an IMBH could alter the orbital properties of the stars that more closely interact with it.

An orbit is a path a unperturbed, collisionless tracer particle (e.g. a star) will move along in a gravitational potential. Orbits contain information about the gravitational potential generated by the mass distribution of a system in their position and velocity coordinates following Newtons 2nd law. Orbit distribution functions (DFs) describe which orbits are populated by how many tracers. From the orbit distribution function together with the overall potential we can draw inferences about the structure and evolution history of the system.

Historically observations of orbits enabled discoveries or confirmed them:

- Seen from the earth Mars' position moves over the sky as a loop called epicycle. That implies that the earth is not the centre of the universe! (**?**, p.3)
- Neptune/Uranus noch mal nachlesen

- From rotation curves of galaxies we see that stars move faster than what expected by the presence of only the mass of luminous matter. There has to be more matter interacting via gravitational forces. This has led to the theory of dark matter. (Rubin 1980)

- Mercury's orbit differs hugely from calculated Kepler orbit. This is because of its migrating pericentre. Due to the proximity to the sun gravitational forces are so strong that we need to apply general relativity.

- The SMBH Sagittarius A* was detected by observations of the orbits around the black hole and resulting mass calculations. (**?**, p.923)

Some examples for orbit DFs are spiral galaxies where stars of different components (thin disc, thick disc, bulge, halo) are on different orbits (dynamical distinct) and have different metallicities (chemical distinct).

Actions are integrals of motion and are the distinct description of orbits. They are constant with time. Known for a long time they are extremly difficult to calculate. Actions of our solar system can be calculated more easily since the potential is a Kepler potential. With nowadays supercomputers it is finally possible to compute actions of more complex and less explored systems. how to describe orbits
idea 1 (x(t),v(t)) pretty complicated time evolution in 6 coordinates. idea 2 take quantities which are constant with time so called integrals of motions
beste set von integrals of motions are actions good to interpret

In this thesis we wish to test the feasibility of the analysis of the action/orbit space in GCs and test whether it could be possible to predict signatures of IMBHs. This will be done by "translating" the traditional phase-space into orbit space, exploiting the potential and the $\vec{x}$ and $\vec{v}$ vectors. Although this type of information (6-D info) is not currently available for Galactic GCs we are motivated by the growing amount of photometric and kinematic data that are already able to deliver a 5-D info (2D spatial info and 3D kinematic info), in particular the high accuracy Hubble Space Telescope (HST) proper motions and the upcoming GAIA data. We will limit our analysis to GC simulations with and without IMBHs to explore our new approach. The thesis is structural in to parts: first we familiarize with a phase space analysis of the simulations and we will focus in how to study the orbits and extract predictions of the presence of an IMBH.

2 Method & Theory

2.1 Stellar population in GC

The typical stellar components of a GC can be seen in a color magnitude diagram (CMD). In this CMD the visual magnitude is plotted against the B-V color. It's color coded by the mass of the star. A star's position can be interpreted as its evolution stage. Most of

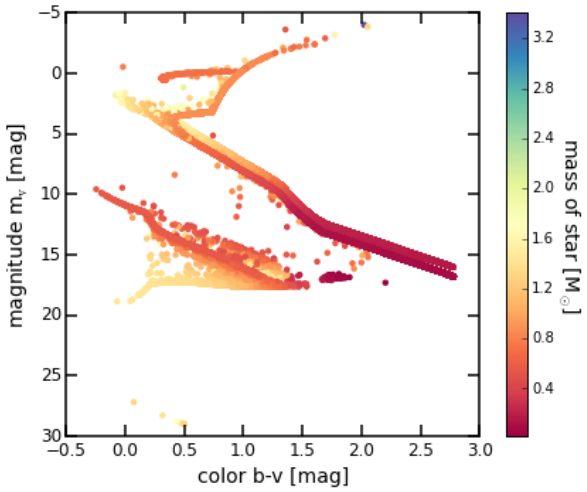

Figure 2: Color magnitude diagram of SIM 1.

the stars are set in the main sequence. They fusion hydrogen in their cores. There are two main sequence lines one upon the other. These occur due to binary systems whose flux is given by the sum of the single fluxes of the single components, and therefore appear redder and more luminous. These binary systems represent about 5% of the stars in the GC. The position of the main sequence turn-off depends on the age of the system and therefore can be used as an indicator to determine the cluster's age. explain isochrones Bluewards of this turn off point following the trend of main sequence stars, there are so called "blue stragglers" which are remnants of stellar collisions or interacting binaries (B&T p.628). Continuing from the turn off point there is the red giant branch consisting of stars still fusing hydrogen but only in a shell surrounding a degenerate helium core. They are inflated with a radius much higher than the main sequence stars but have a much lower temperature. These are the brightest stars of a GC. On the upper part of the red giant branch lies the horizontal branch. Its stars burn helium in their core and hydrogen in a surrounding shell. In the lower left corner white dwarfs are located. They are stellar remnants which have burnt all of their resources. In a typical GC dark stellar remnants like stellar black holes and neutron stars are present but not

visualised in the CMD. nochmal über CMD durchlesen

2.2 Kinematic profiles of globular clusters

velocities are gauss distributed assumption Our investigations of GCs in phase space consists in analysing the spatial distribution of stars (density profiles) and the kinematic profiles(such as velocity dispersion and anisotropy profiles). First we test the sphericity of the GC. Sphericity implies the usage of analytical methods that are very straight forward, especially for determing the potential of the globular cluster and then the actions in action space.

density profile

The velocity dispersion is the standard deviation of the mean velocity

$$\sigma_i = \sqrt{\langle (v_i - \langle v_i \rangle)^2 \rangle} = \sqrt{\langle v_i^2 - \langle v_i \rangle^2 \rangle} \qquad i = r, \theta, \phi. \tag{1}$$

For a spherical system it is best to calculate them in spherical coordinates r, θ, ϕ respectively v_r, v_θ, v_ϕ. If the GC contains an IMBH the velocity dispersion towards the centre is expected to increase.

what exactly describes anisotropy? To quantify the anisotropy of the system we use the anisotropy parameter β

$$\beta(r) \equiv 1 - \frac{\sigma_\theta^2(r) + \sigma_\phi^2(r)}{2\sigma_r^2(r)}. \tag{2}$$

If β is positive the anisotropy is radial, if it is negative the anisotropy is tangential and if $\beta \approx 0$ then the system is isotropic.

2.3 Density & potential

2.4 Integrals of motion

2.5 Orbits & orbit integration

how does the orbit in a spherical potential look

include effective potential

In a dynamical system the mass distribution is described by the form of theoretically existent orbits $(\vec{x}(t), \vec{v}(t))$. Position and velocity are linked with six coordinates and contain all information about the potential. With Newton's 2nd law we get the connection

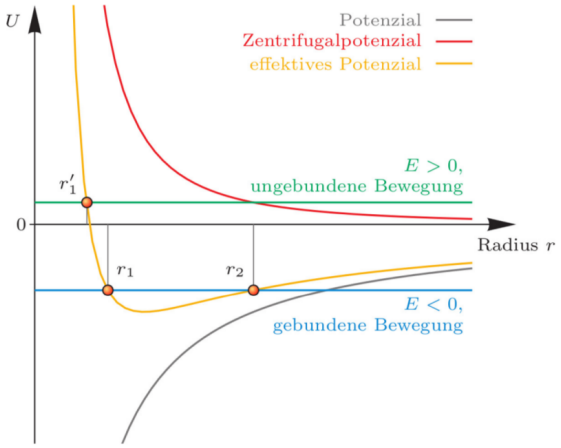

(a) General potential of a central field. The black line is the potential which is the difference between the effective potential (yellow line) and the centrifugal potential (red line). If the effective potential is positive the object is unbound while having a negative potential the object moves on a bound orbit. The points where the effective potential equals the total energy are the peri- and apocentre (r_1 and r_2) of the orbit. The point with the lowest effective potential is the guiding star radius. This is the distance a star with given angular momentum would have on a circular orbit. [Bartelmann Skript Theo 1]

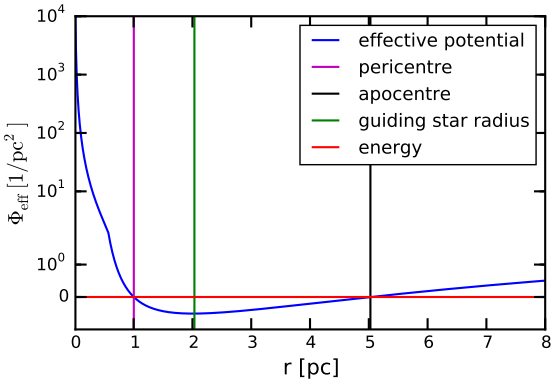

(b) Effective potential of a random star of SIM 1 (blue line). The total energy of the star (red line) is -1.88e-24 pc^2/s^2. The intersections of energy and effective potential are the peri- and the apocentre of the star (magenta and black lines) and the minimum of the effective potential (green line) is the guiding star radius.

Figure 3: Effective potentials.

between potential $\Phi(\vec{r})$and acceleration $\vec{a}$ which is

$$\vec{F}(\vec{r}) = -\nabla\Phi(\vec{r}) = m \cdot \vec{a}.$$

Since the system is spherically potential and force only depend on the distance from the centre r. The potential can be derived from the Poisson's equation

$$\Delta\Phi(r) = 4\pi G\rho(r) \tag{3}$$

with the density ρ depending only on the distance as well. Due to the spherical symmetry the potential can be calculated by

$$\Phi(r) = -\frac{G}{r}\int_0^r \mathrm{d}M(r') - G\int_r^\infty \frac{\mathrm{d}M(r')}{r'} = -4\pi G\left[\frac{1}{r}\int_0^r \mathrm{d}r' r'^2\rho(r') + \int_r^\infty \mathrm{d}r' r'\rho(r')\right] \tag{4}$$

(Binney & Tremaine eq. 2.28). We calculate the density by binning the masses on logarithmic equally distributed shells write density formula? and solve the integrals of the Poisson's equation numerically by using the Gauss-Legendre quadrature

$$\int_a^b f(x)dx = \frac{b-a}{2}\sum_{i=1}^{n} w_i f\left(\frac{b-a}{2}x_i + \frac{a+b}{2}\right)$$

where the points x_i and the weights w_i are derived from the Legendre polynomials. Since the orbit is described by position and velocity at each time step we use the numerical leapfrog method which is a second-order time reversible integrator. X_i and v_i are calculated by

$$x_{i+1} = x_i + v_i\Delta t + \frac{a_i(x_i)}{2}\Delta t^2$$
$$v_{i+1} = v_i + \frac{a(x_{i+1}) + a(x_i)}{2}\Delta t.$$

gcs are collisional clusters but we assume them as collisionless
time evolution of actions

2.6 Actions

Stars in spherical symmetric potential are fully described by their actions

$$J_i = \frac{1}{2\pi} \oint_{\gamma_i} \vec{p} \cdot d\vec{q} \qquad\qquad i = r, \theta, \phi \tag{5}$$

which are used as coordinates in action space These actions are integrals of motion. For most potentials actions can't be described analytically. The actions of a spherical system are derived from angular momentum, energy and potential. Only the potential is depending in r. Energy and angular momentum as well as resulting actions are constant over time and orbit. The azimuthal action J_ϕ and the latitudinal action J_θ can be evaluated simply. To calculate the radial action J_r we have to solve an integral numerically. Actions of a spherical potential are found to be

$$J_\phi = L_z, \tag{6}$$

$$J_\theta = L - |L_z|, \tag{7}$$

$$J_r = \frac{1}{\pi} \int_{r_{min}}^{r_{max}} \mathrm{d}r \sqrt{2E - 2\Phi(r) - \frac{L^2}{r^2}}. \tag{8}$$

Should I write down the derivation of the actions (B&T p.220) or just the results (B&T p.221, 3.221,3.223,3.224)?

The pericenter r_{min} and the apocenter r_{max} as well as the guiding star radius r_g can be found in the effective potential

$$V_L(r) = V(r) + \frac{L^2}{2mr^2}. \text{ m should be left out right?} \tag{9}$$

Bartelman Theo 1 Skript p59 formula 6.27.

In the peri- and apocenter the effective potential equals the total energy since the stars do not have any kinetic energy there. That results in following function which is to solve:

$$\left(\frac{1}{r}\right)^2 + \frac{2 \cdot (\Phi - E)}{L^2} = 0.$$

The guiding star radius is the distance at which a star with given total angular momentum would have a circular orbit. This is at the minimum of the effective potential. To

get r_g we have to solve

$$r\sqrt{r\frac{\partial\Phi}{\partial r}} - |L| = 0$$

where $\sqrt{r\frac{\partial\Phi}{\partial r}} = v_{circ}$ is the circular velocity. This distance is used to have a better comparison of the actions since in the snapshot the stars are at a random position on their orbit.

plot v_eff plot from barthelman skript?

3 Analysis

3.1 Description of the simulation

Name of the simulation	Number of particles	Total mass [$M_\odot$]	Mass of the IMBH [$M_\odot$]	r_m [pc]	Age [Gyr]
SIM 1 - IMBH	1026735	$3.09 \cdot 10^5$	10102	4.13	10
SIM 2 - IMBH	1079376	$3.26 \cdot 10^5$	8902.3	3.58	7
SIM 3 - NOIMBH	468627	$1.73 \cdot 10^5$	0	7.89	11
SIM 4 - NOIMBH	1851556	$6.70 \cdot 10^5$	0	5.41	11

Table 1: Overview of the data of the simulations. We show the basic properties of each simulation which are numper of particles, the total mass, the mass of the IMBH, the half mass radius and the age. The half mass radius is defined by the radius which includes half of the mass of the whole system.

where simulation comes from and what it is & description of output

To get familiar with the simulation we first have a look at the scatter plot of the star positions.

include same plot with velocities!!

As we said in section **??** it is important to test the sphericity of a system. We will do this by splitting the GC into octants and compare their mass or number since we will introduce mass density plots only later density mass density sphericity plots. As you see they're acceptable overlaying within their errors.

As mentioned in **??** the CMD is showing a star's evolution stage dependend on its position. If you do not know age or metallicity of the system you can fit isochrones on the CMD. Isochrones are curves of evolutionary stages of stars having the same age and metallicity but different masses. We plot several to our CMD to determine which one fits best. This will give us the age and the metallicity of the system.

3.2 Investigation in phase space

First we will investigate the GC in phase space for the set of simulations that w will use throughout this work. We will start with the velocity dispersion and the anisotropy parameter then we will have a density profile and from that get the potential. for all 4 simulations or only for the first with IMBH? or with on plot containing two or all of them?

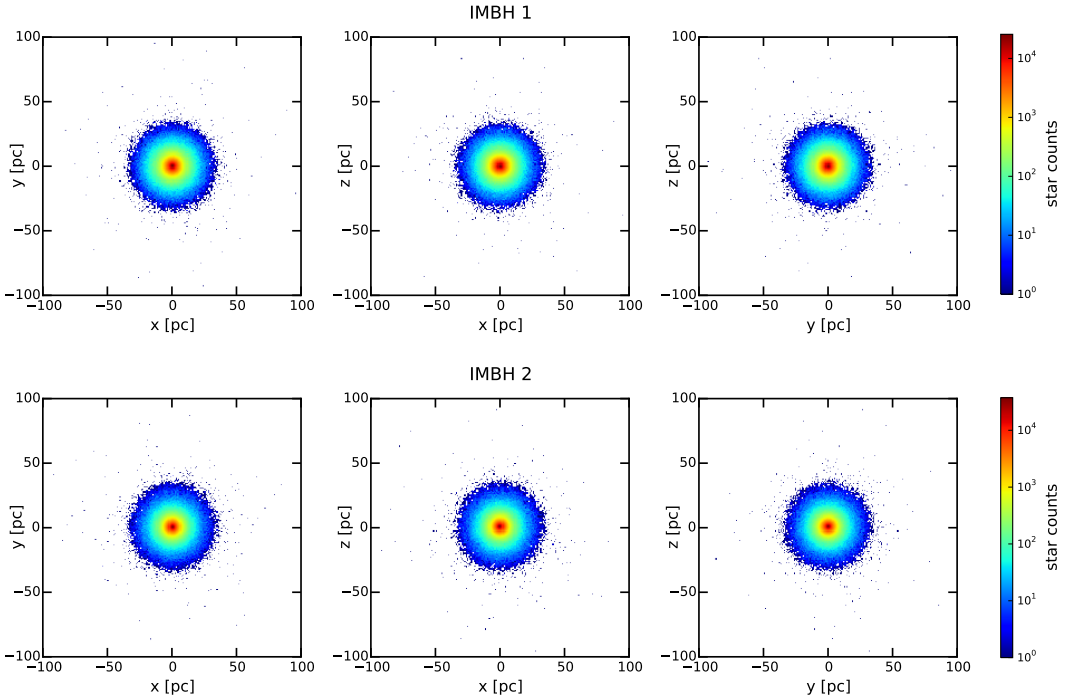

(a) SIM 1. The GCs are spread until 100 pc with most of the stars located in the inner 40 pc.

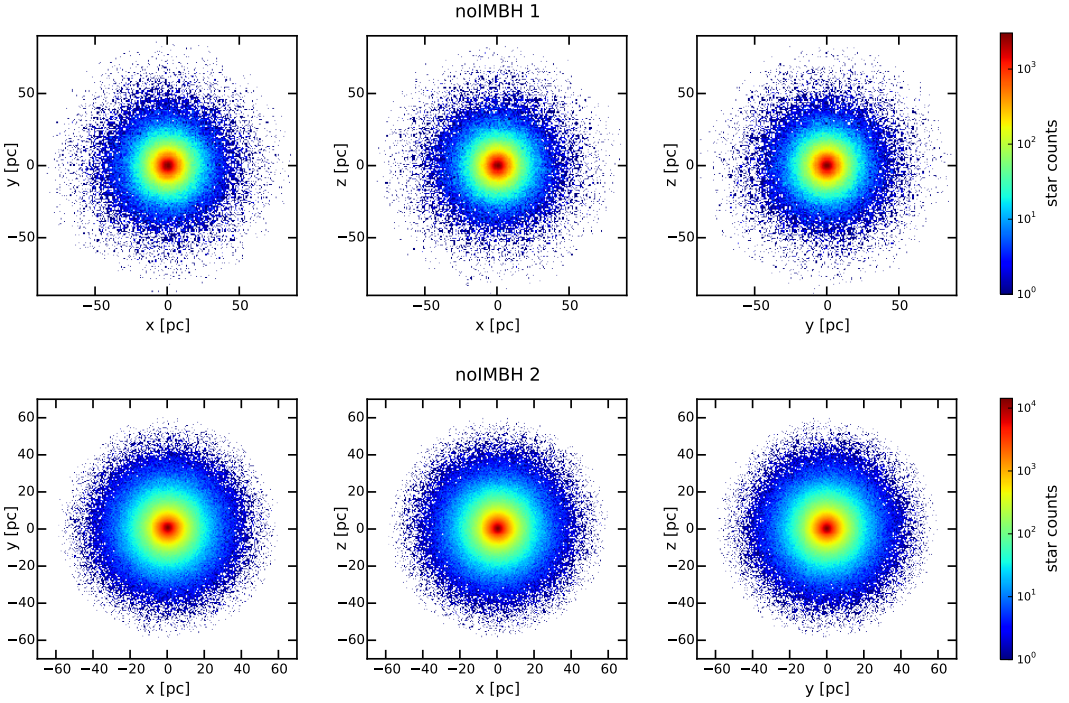

(b) SIM 3. The GC is spread until 90 pc (SIM3) and until 60 pc (SIM4).

Figure 4: Position scatter plots. The stars are distributed spherically with most of the stars in the inner part. The stars of the GCs with IMBH are less spread in the outer parts despite very few which are far outside. In the GCs without IMBH the stars in the outer part are less accumulated but the furthermost stars still in the main sphere.

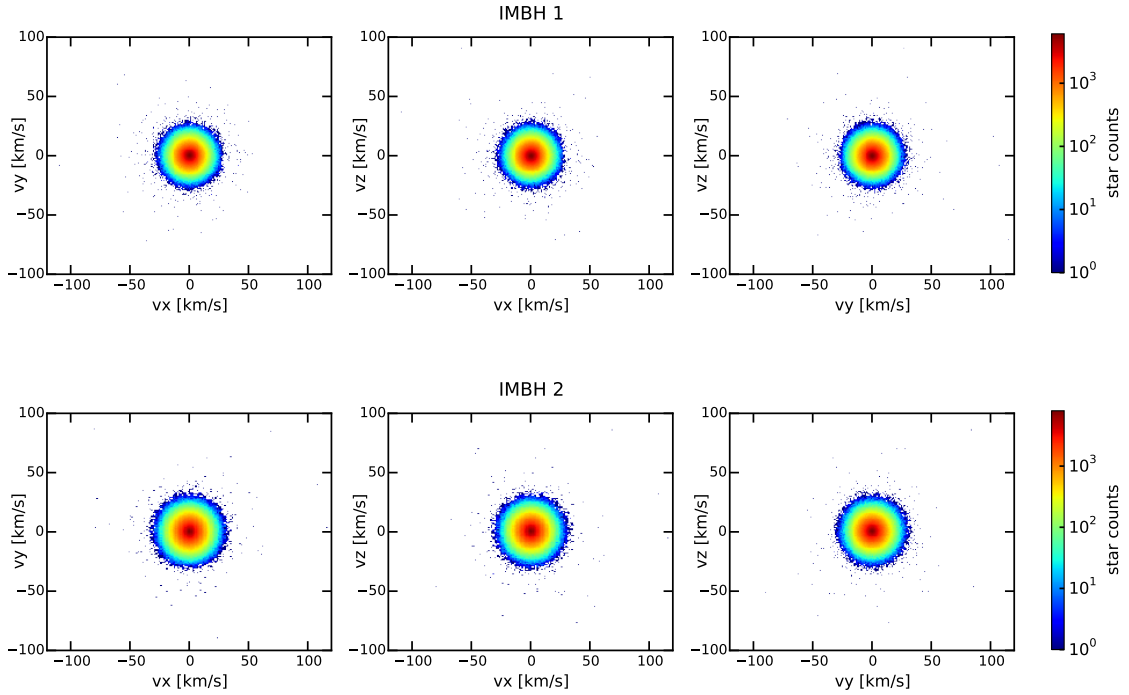

(a) SIM 1. The stars' velocities are spread until 120 km/s with most of them reaching 30 km/s.

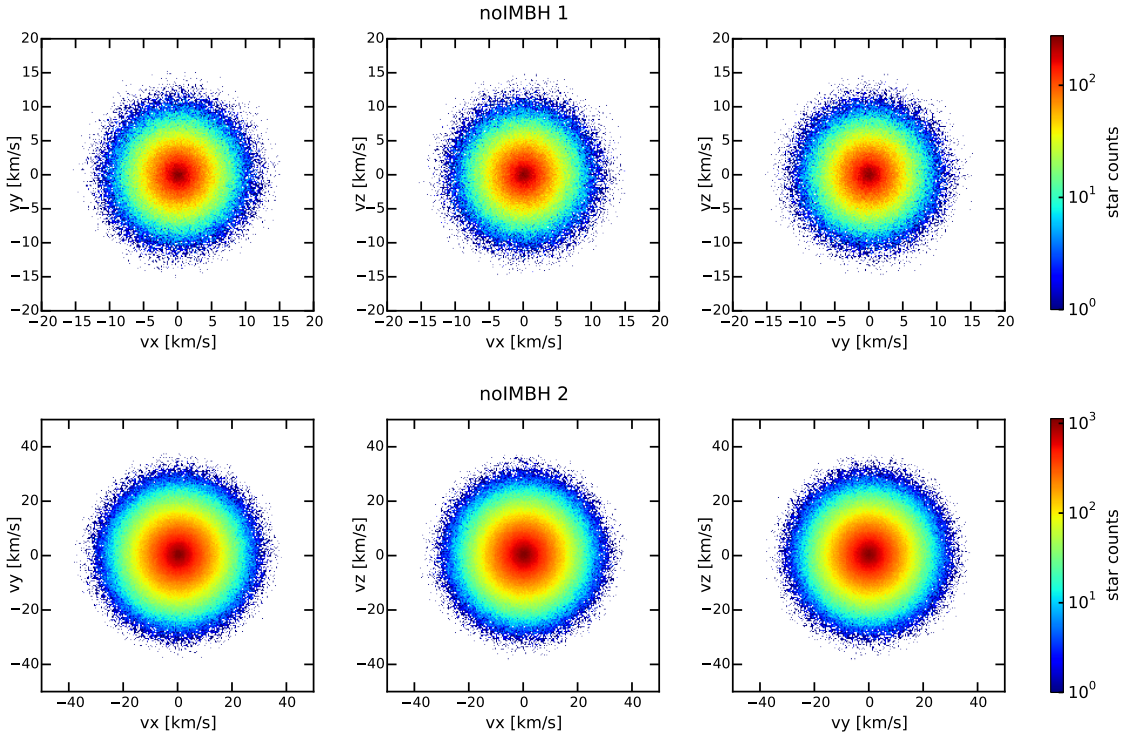

(b) SIM 3. The stars' velocities are spread until 15 km/s for SIM 3 whereas they spread until 40 km/s for SIM 4.

Figure 5: Velocity scatter plots. The velocities are spherically distributed. Most of the stars have low or no velocity while a few have high velocities in different directions. Like the star distributions the velocity distributions of the GCs with IMBH have some velocities outside the main sphere whereas the GCs without IMBH contain all velocities inside the main shell.

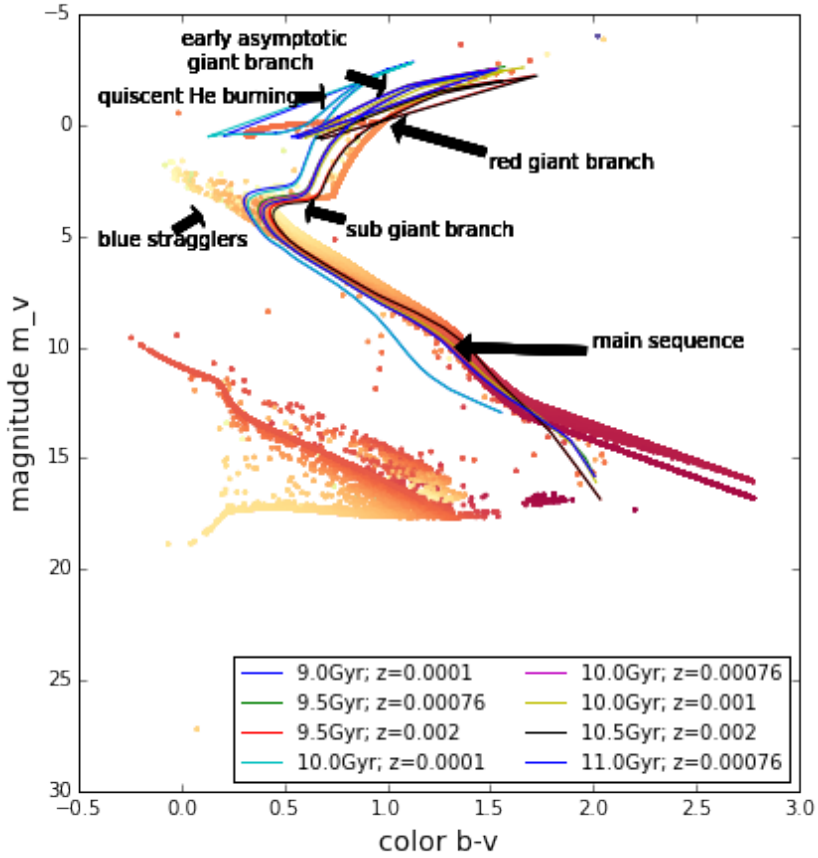

Figure 6: Color magnitude diagram of SIM 1 overplotted with different isochrones. We recognize how we can determine the age based on the turn off point. This verifies the age and the metallicity of this GC of 10 Gyr and 0.001.

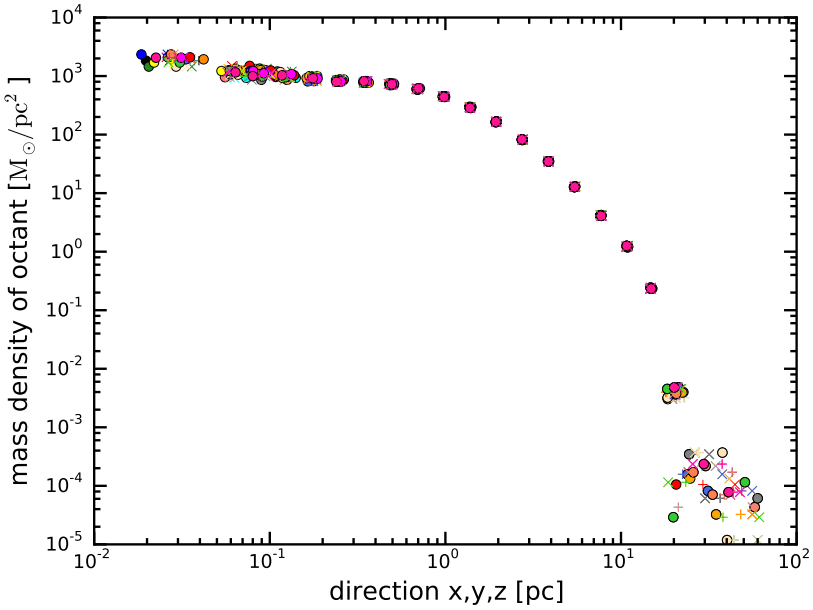

Figure 7: Test for sphericity and center of mass of SIM 1.

3.2.1 Velocity dispersion

With (1) from section **??** we can calculate the velocity dispersion for each coordinate r, θ, ϕ. For every bin we take the same amount of stars and calculate the dispersion. To compare both simulations we plot the dispersion over the effective radius. The half mass radius of the simulation with IMBH is 4.1pc and of the simulation without IMBH it is 7.9pc. As expected there is a rise in the centre for the simulation with IMBH. This is due the high gravitational potential of the IMBH which disturbs the dynamics of close stars.

3.2.2 Anisotropy

Anisotropy can be calculated from (2) in **??**. It is binned the same way as for the velocity dispersion and again dependent on the effective radii. In the center of both GCs there is nearly the same anisotropy. Both are positive and rising. That means the systems are radial anisotropic. The GC with IMBH is most radial anisotropic in its center at about 4 effective radii. The other GC is becoming more radial anisotropic the more far from the centre it is.

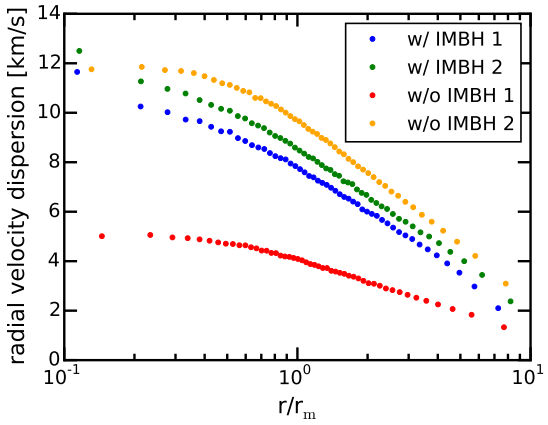

(a) Radial velocity dispersions

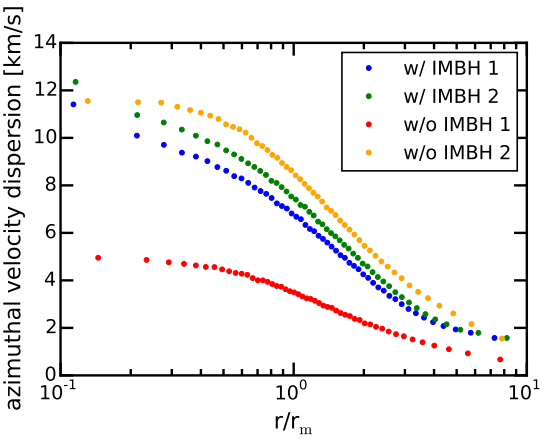

(b) Azimuthal velocity dispersions

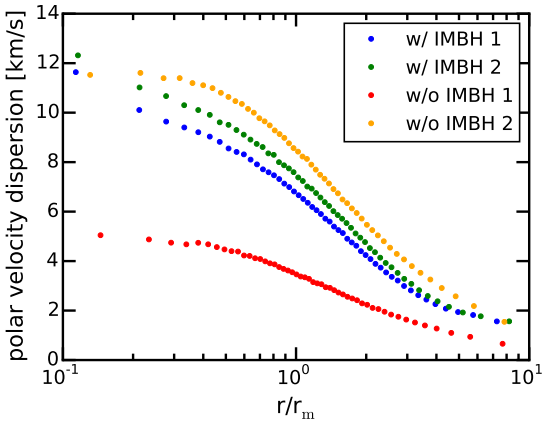

(c) Polar velocity dispersions

Figure 8: Velocity dispersion profiles as a function of the radius in units of the effective radius r_{eff}. They are binned in a way that each bin contains the same amount of stars. We can see that the velocity dispersion of the simulation with IMBH rises towards the centre whereas the simulation without IMBH exhibits a cored profile.

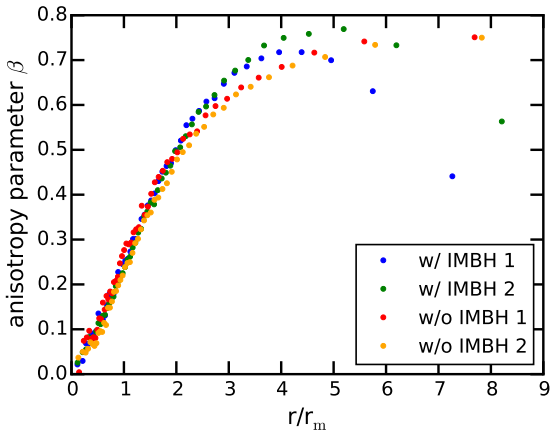

Figure 9: Anisotropy parameter β. All simulations are radial anisotropic. The simulations with IMBHs have a peak at 4 and 5 effective radii where they are most radial anisotropic. The other simulations are rising until the end. The far more outside a star is the higher its radial anisotropy is. Within the first two effective radii all seem to have the same course.

3.2.3 Density profile

The density profile shows the density of the system over its radius. The bins are chosen so that the radii are equidistant on a logarithmic scale and that they are at least 100 stars per bin to have a reliable stochastic. Outside of the cluster the density is set to 0. In the innermost part the density is set to be as the innermost point. plots

3.2.4 Potential

From the density profile we can compute the potential as described in 2.3. It is composed by the potential given from the stars and if there is one the potential of the IMBH expressed as Kepler potential.

3.3 Investigations of orbits in action space

wilma class

3.3.1 Orbits & actions

3.3.2 Integral of motions along orbits

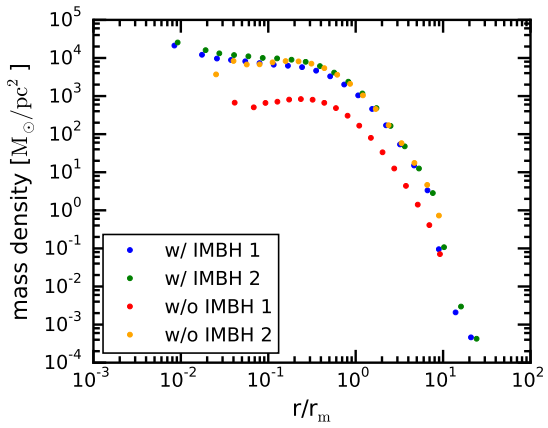

(a) Mass density profiles of all four simulations.

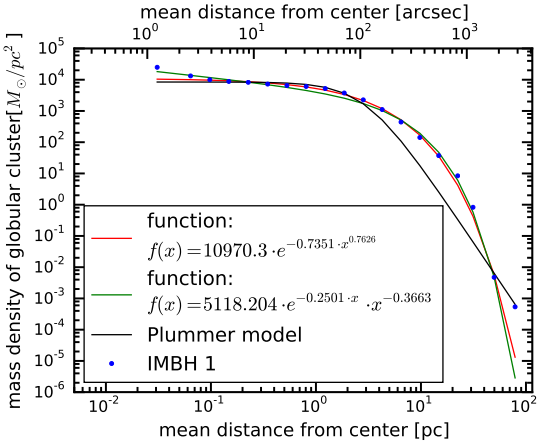

(b) Analytically fitted mass density profile of SIM 1.

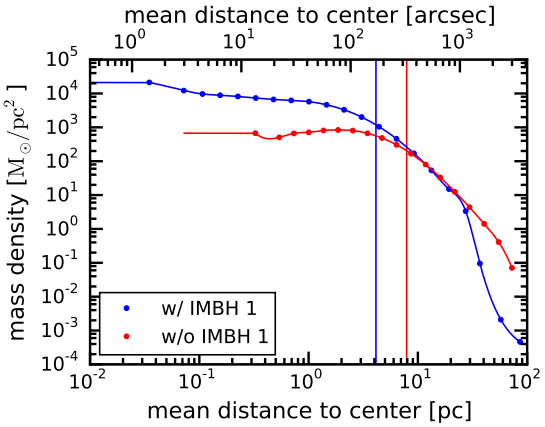

(c) Interpolated mass density profiles of SIM 1 and SIM 3.

Figure 10: Mass density profiles. The density in $\frac{M_\odot}{pc^2}$ is plotted against the effective radius. The density of the GC with IMBH is everywhere larger than the density of the GC without IMBH. In the centre there is a raise in the density of the GC with IMBH whereas the other GC stays approximately on the same level. Both start decreasing at about 0.5 r$_e$ff. We can see in 10c that it is not simple to find an analytical function describing the density. Thats why we interpolate it in 10c. Everything out of the GC is set to 0 while the innerst density is set to be the value of the innermost point.

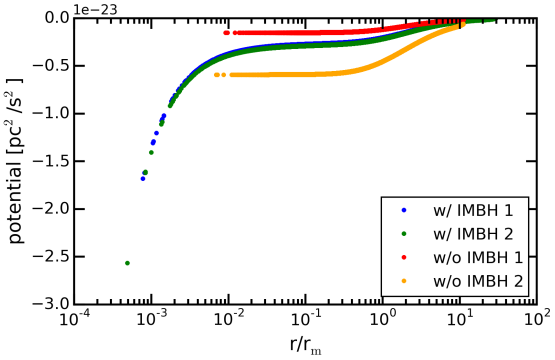

Figure 11: Potential of all GCs. SIM 1 and SIM 2 are nearly overlaying. They are the same simulation at different ages. The simulation lost 5 % of its stars with 10 % of the total mass while the IMBH gained 13 %. The potential of the stars declines while the potential of the IMBH rises so the potential stays the same. The GCs without IMBH remain constant in the inner part (until 0.5 half mass radii) and decrease from the points where their densities decrease.

4 Results & Discussion

only triangle plots

4.1 Signatures of IMBHs in action space

After investigating the orbits at given actions and the time evolution of the integrals of motion we consider all actions and other integrals of motion at our given snapshots. We have a look at the energies and angular momenta of the stars and compare them with the radial actions. Our main goal is to find any systematic signatures for the simulations with IMBHs that can be considered as the direct evidence of the dynamical effect of the IMBH itself. For this reason we investigate selected stars which show an abnormal behaviour in above-mentioned plots and compare them to the rest of the data to see where we find them.

In 12 we plot the radial action over the energy of the star as histograms for all GCs. We see clearly some stars outside of the moon shape. They have either no radial action and high energy(below $-4 \cdot 10^{-24}$ pc^2/s^2) or nearly no energy and high radial action (above 500 pc km/s).

We check the effective potential of the stars of the group to get information of their orbits and their actual positions. In 13 show one exemplary graph for each group taken from SIM 1.

The first group of stars of SIM 1 contains 38 of the nearest 110 stars including the innermost 15 stars. Since they have really low (nearly 0) radial actions they are on circular orbits. The nearest 15 on circular orbits around the IMBH are certainly locked to the IMBH. That is why we do not see this signature for SIM 3 and SIM 4. The other stars of this group are likely to be locked to the IMBH as well while the rest of the near stars which are not in this group seem to be near to or in their pericentre on more elliptic orbits and therefore not locked to the IMBH.

The other group of stars with high radial actions and nearly no energy can not be clearly related to the IMBH. They are the furthermost stars of the snapshot. All are in their apocentre on very elliptic orbits (calculate ellipticity?). This ellipticity could be caused by the IMBH but since most of their pericentres are at a few pc we can not assume much interaction with the IMBH for those stars. Another reason that these stars do not occur in this way in SIM 3 and SIM 4 can be due to different truncation prescriptions used in the simulations (see graph 9). These stars are nearly outside of the GCs and have about zero energy so they could have been excluded in SIM 3 and SIM 4.

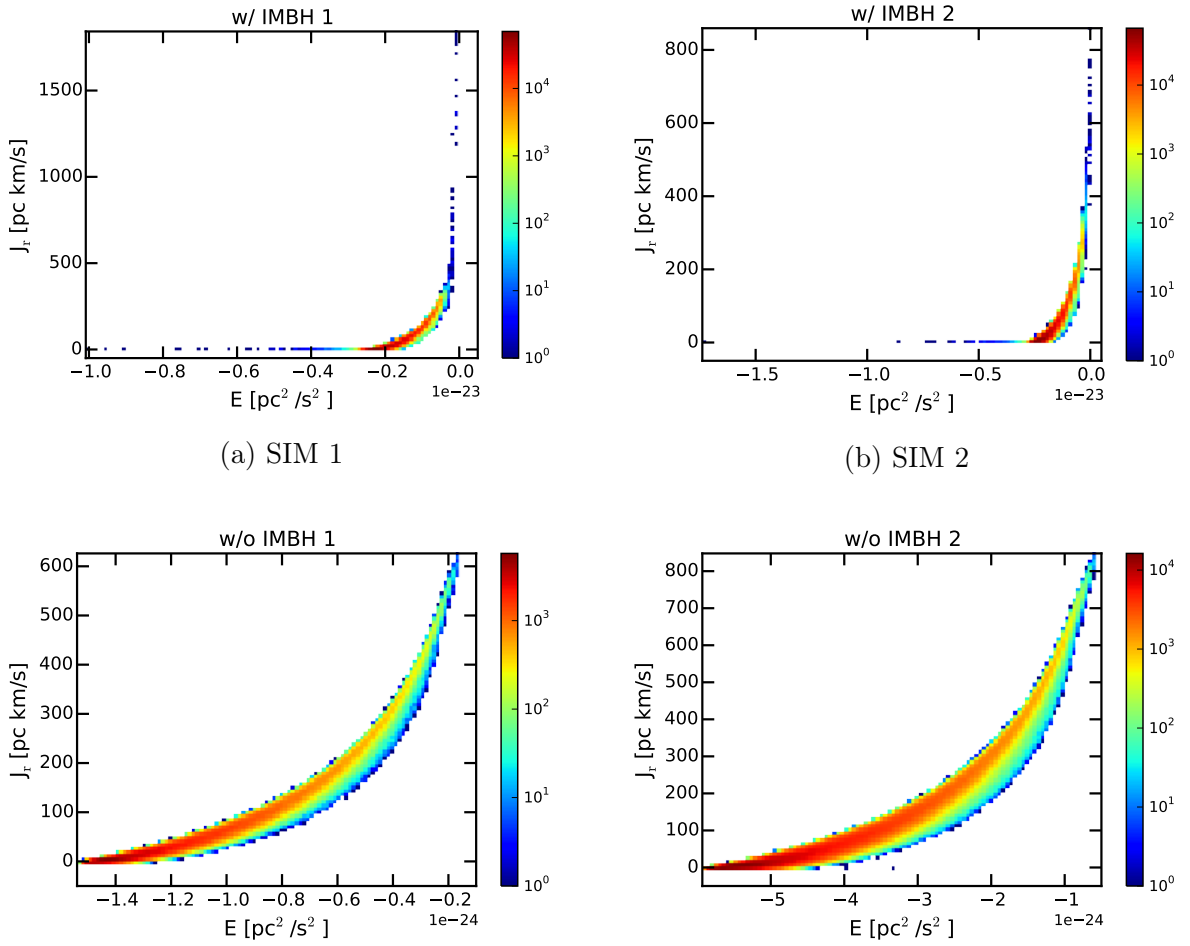

(a) SIM 1

(b) SIM 2

(c) SIM 3

(d) SIM 4

Figure 12: Radial action over energy. In 12a and 12b it is plotted for both simulations with IMBH and the lower ones are for the simulation without IMBH. We find the crescent shape from 12c and 12d clearly in 12a and 12b. But in SIM 1 and SIM 2 there are some stars differing from this shape. Some have high energy with no radial actions (henceforth referred to as group 1) while others have high radial actions with nearly no energy (henceforth group 2).

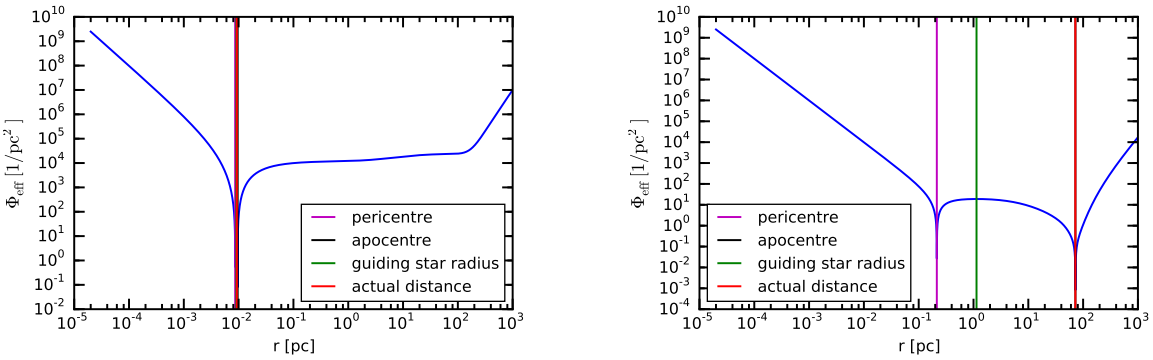

(a) Star of group 1

(b) Star of group 2

Figure 13: Effective potential of exemplary stars of both groups from figure 12. The star of group 1 is clearly one a circular orbit with $r_{min} \approx r_g \approx r \approx r_{max}$. The star of group two has a highly eccentric orbit and its actual position is in its apocentre.

We might get these high energies from former binaries which were divided earlier. One of the stars could have been captured on a circular orbit near the centre while the other could have been left on an unbound orbit and have left the system. To check this we will plot the same values only for our actual binary systems. As we see in 14 the binary systems are behaving like single stars. There is no signature that the divergent stars are leftovers of former binaries.

Next we plot the radial actions over the absolute angular momenta of the stars of the simulations again as histograms. In 15 we can see a triangular shape which seems characteristic. Inside this shape we see some substructure in the GCs with IMBH. The stars outside the shape are the stars of group 2 which we see in 12 and 14 as the stars with no energy and high radial actions. Obviously they don't seem to have a specific angular momentum. We do not know how to identify the stars in the substructure. There could be a mass-dependent correlation due to dynamical mass segregation.

We extract these divergent stars and determine their properties. First we check the positions of their actions depending on their guiding star radii. In graph 17 the radial actions are plotted over their guiding star distances. We highlight the stars of group 1 and group 2 taken from graph 12 for SIM 1 and SIM 2. In general, there are several stars which have a really small guiding star radius (up to $10^{-}5$ pc). In SIM 3 and SIM 4 only very few stars go below 0.1 pc. Another difference between the GCs with and the ones without IMBH is that on the right border the lower end goes until very low radial actions for SIM 1 and SIM 2 (up to $10^{-}6$ pc km/s) while SIM 3 and SIM 4 end there

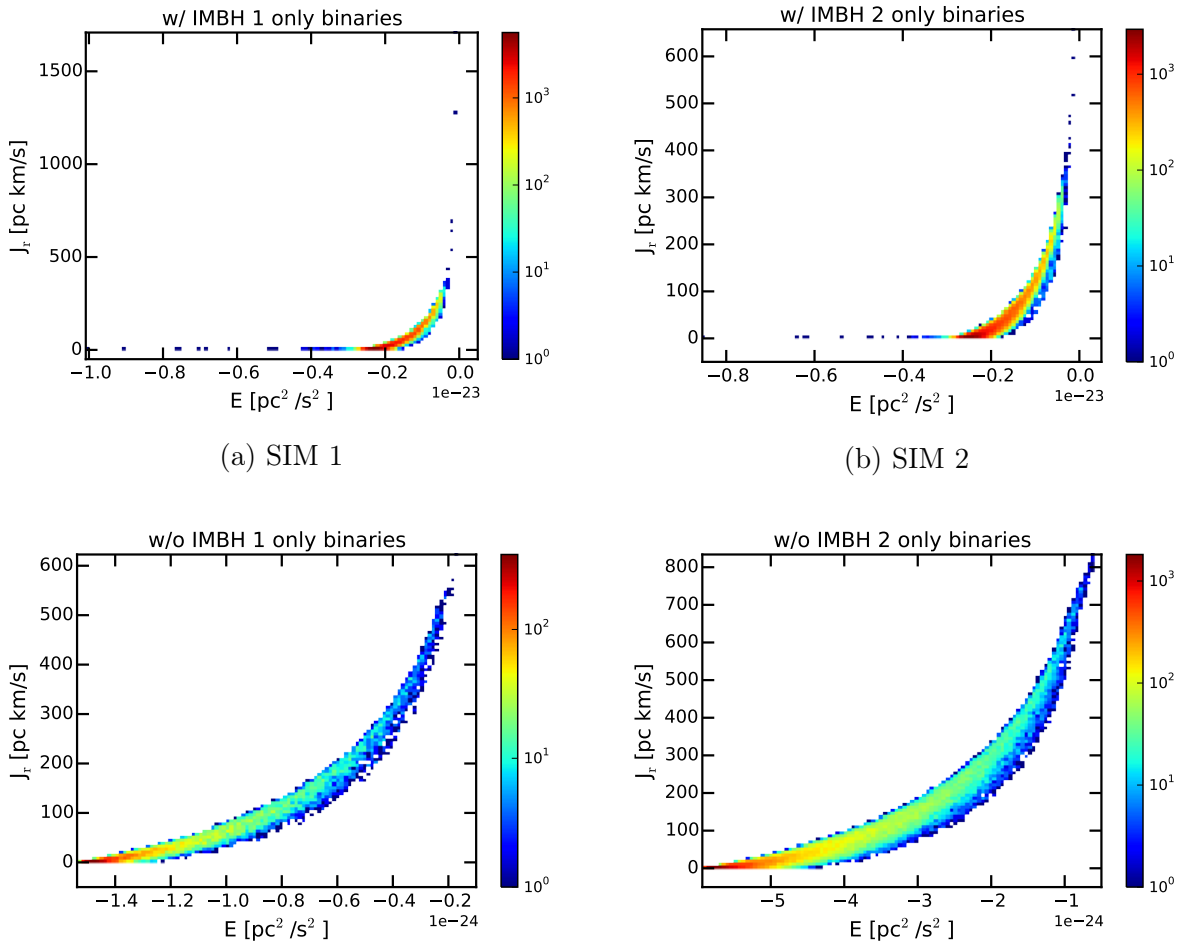

(a) SIM 1

(b) SIM 2

(c) SIM 3

(d) SIM 4

Figure 14: Radial action over energy only of binary systems. We see the same distribution of stars as in 12.

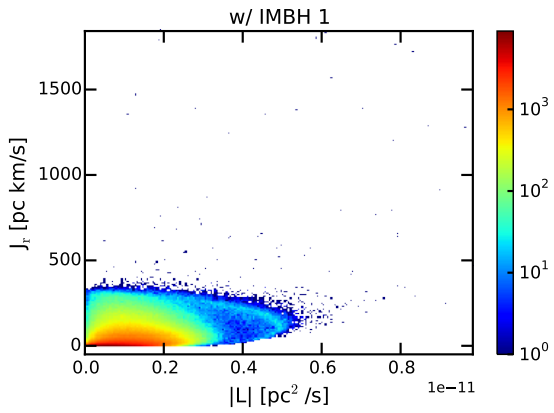

(a) SIM 1

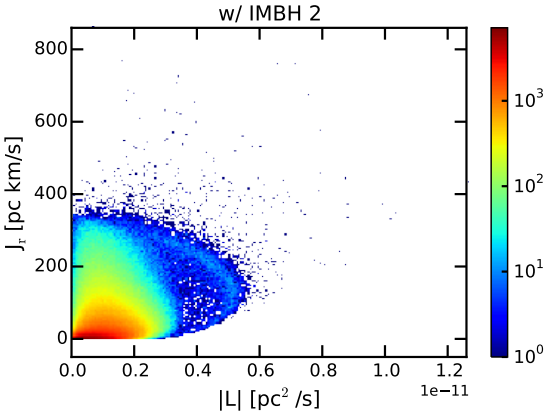

(b) SIM 2

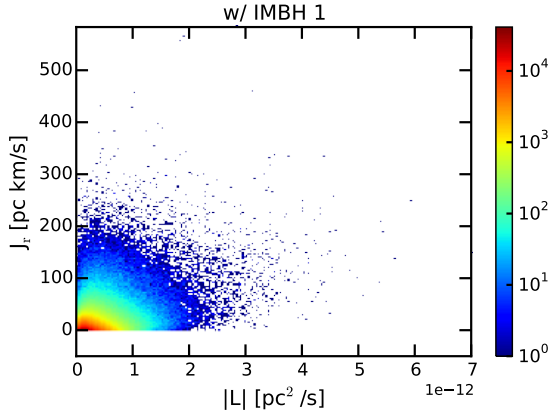

(c) SIM 1 mass weighted

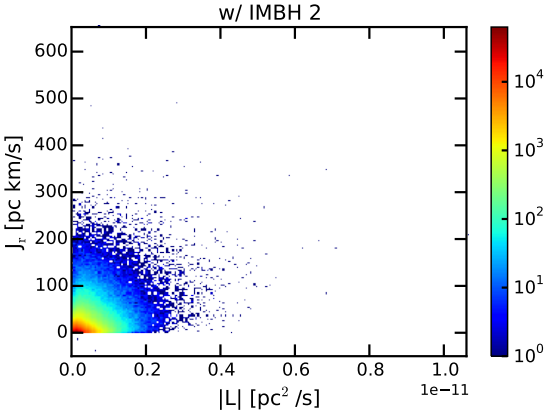

(d) SIM 2 mass weighted

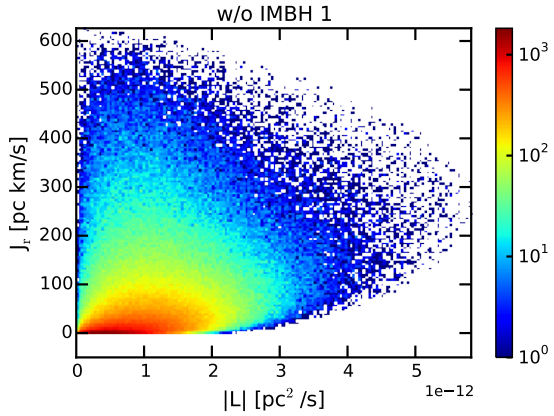

(e) SIM 3

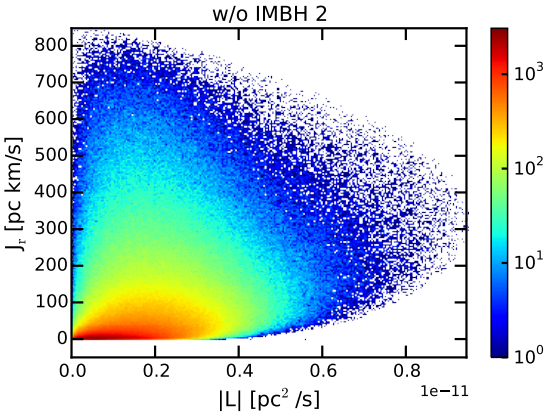

(f) SIM 4

Figure 15: Radial action over angular momentum. 15e and 15f look again very similar to each other with no recognizable substructure. In 15a and 15b there are stars above the main shape. In the shape we can clearly see a substructure from about 0.3 to about 0.5 pc^2/s in nearly the whole radial action range. half moon not directly spatially connected to imbh (plot mit color coding pericentre einfügen) probably only specific to the simulation

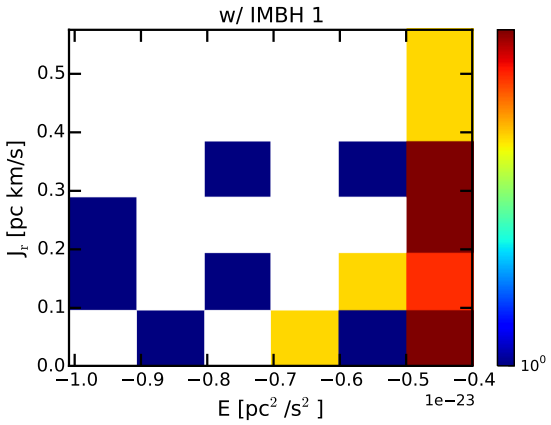

(a) Radial action over energy only for IMBH influenced stars of SIM 1.

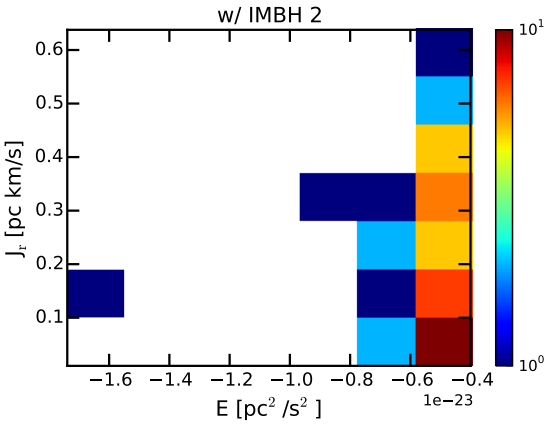

(b) Radial action over energy only for IMBH influenced stars of SIM 2.

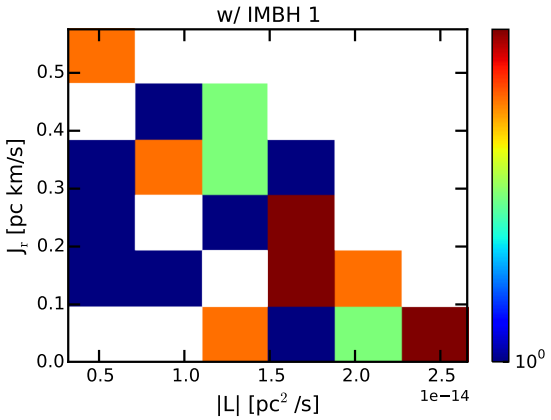

(c) Radial action over angular momentum only for IMBH influenced stars of SIM 1.

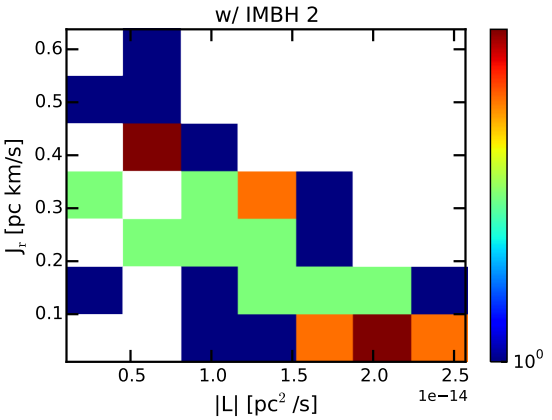

(d) Radial action over angular momentum only for IMBH influenced stars of SIM 2.

Figure 16: Check for group 1 stars.

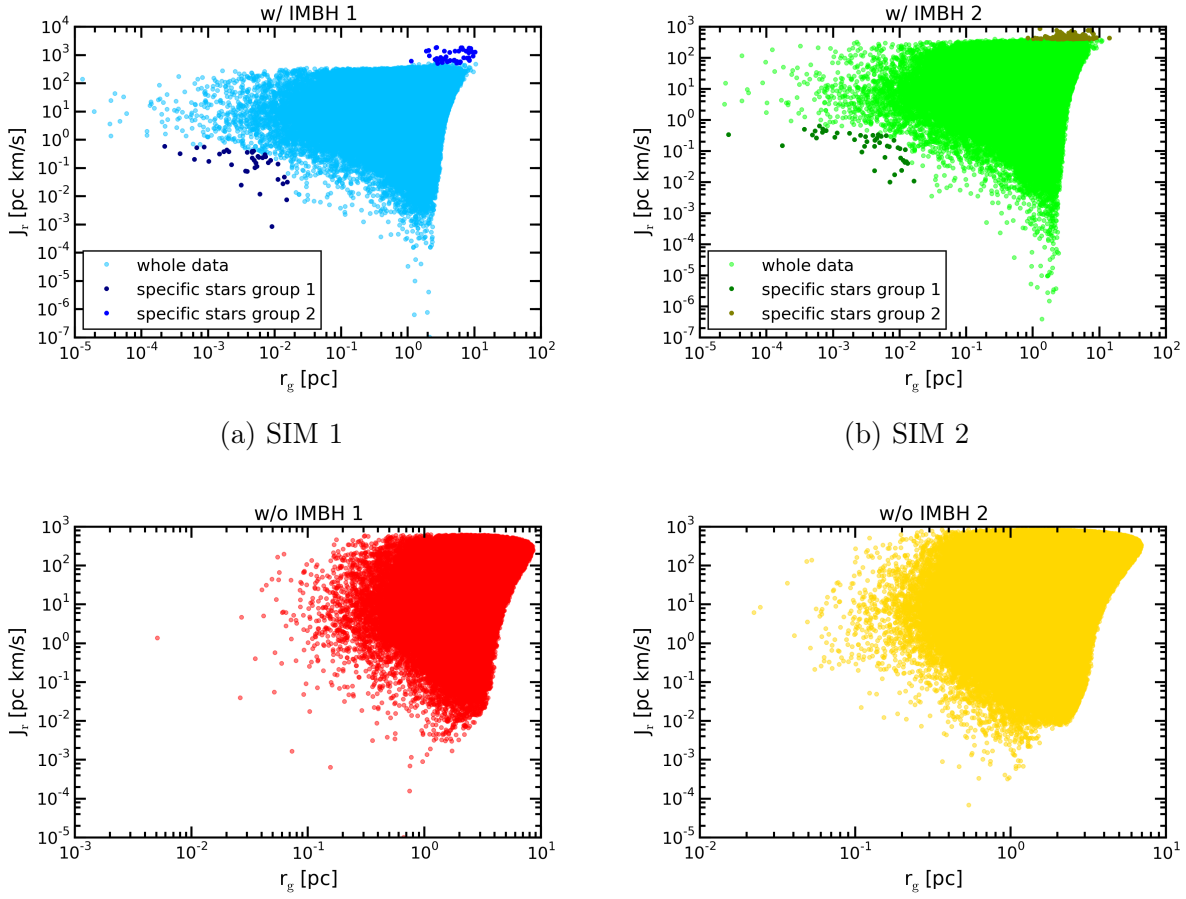

(a) SIM 1

(b) SIM 2

(c) SIM 3

(d) SIM 4

Figure 17: Radial action over guiding star radius with marked specific stars on loglog scale. All simulations have a similar shaped distributions except for the marked stars which are the specific ones. On the top right corner the shape of 12a and 12b is not gently rounded but there are single stars around it. On the lower left there are some extra stars which we identify as the stars with low radial action.

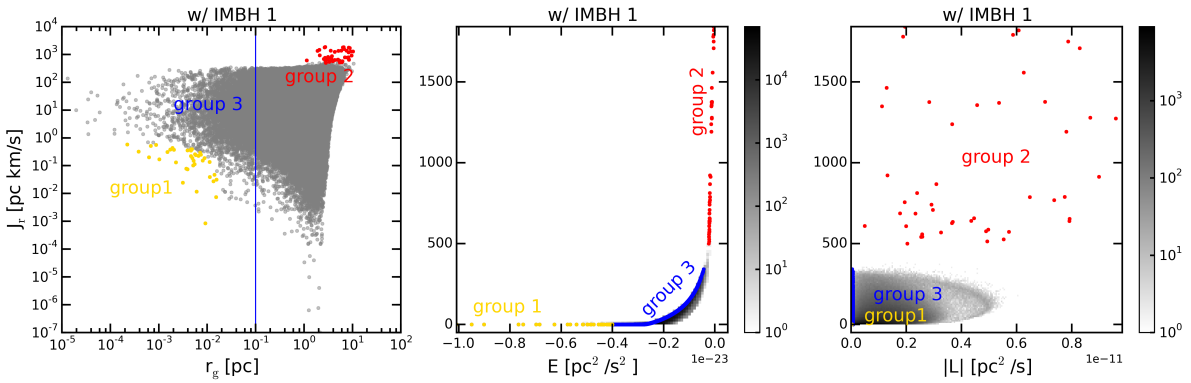

Figure 18: Radial action over different values.

softly at about 10^-2 pc km/s. We investigate these different stars again in the radial action over energy plot to check their properties by colorcoding these different parts.

In figure **??** we can match the different parts of figure 17. The grey part of figures **??** and **??** is the whole data color coded by the pericentre. The yellow to red part is the part where the guiding star radius is smaller than 0.1 pc again color coded by the pericentre. The green stars are the stars of group 2 while the pink stars contain stars of group 1. The blue stars are star with a high angular momentum (bigger than $7 \cdot 10^{-12}$ pc^2/s). If we subtract all color coded stars from this plot we get approximately the shape of SIM 3 and SIM 4.

4.2 Discussion & future perspectives

In summary we can say that we found clearly evidence of the IMBH in the radial actions. To get there we made some simplified assumptions which should be investigated more precisely in an extended work. The density is the basis of our approach of the actions. Since we didn't find an analytical function we interpolated the binned densities and set the central density equal to the innermost density bin. Another attempt to get the density could be done by modelling Multi-Gaussian Expansion to the graph. But for this thesis we see the interpolation as sufficient since tests with some different densities do not destroy the figures of section 4.1.

Additional inaccuracy of the results rises due to different simulations for GCs with and without IMBH. Since they have different initial conditions and conditions throughout the simulating process we can not compare them directly. Especially the radial actions can not be compared since they are mass dependent. We see the differences directly in the scatter plots (figures 4 and 5) and in the anisotropy due to different truncation

prescriptions. In further investigations we should consider using simulations with same conditions despite only the absence of an IMBH in one of the simulations.

Some physical assumptions have been that actions stay totally constant over time or rather that we have only looked at them at the time of the snapshot (despite a few stars for which we integrated the orbit and have looked at the time evolution of their integrals of orbits). Changing integrals of motion go along with changing orbits which could have some numerical fluctuations especially near the IMBH.

Another assumption is that we use specific values if not said else. That means we divide all values by the mass of the stars. We see in fig 15 that there can be distortion due to that. Further work can investigate the mass dependency of the integrals of motion.

If all these points are applied to this method we should think of a way to apply this approach to observational-like data. The main difference is that at this moment there is no possibility to get the masses of the stars of GCs and therefore we can not derive the potential which is essential for this method.

5 Conclusion

6 Acronyms

CMD color magnitude diagram

DF distribution function

GC globular cluster

HST Hubble Space Telescope

IMBH intermediate mass black hole

MW Milky Way

SMBH super massive black hole